ESC European Society of Cardiology

European Heart Journal - Cardiovascular Imaging (2019) **20**, 990–1003
doi:10.1093/ehjci/jez068

Focal scar and diffuse myocardial fibrosis are independent imaging markers in repaired tetralogy of Fallot

Hubert Cochet[1,2*†], Xavier Iriart[3†], Antoine Allain-Nicolaï[1], Claudia Camaioni[1], Soumaya Sridi[1], Hubert Nivet[1], Emmanuelle Fournier[3], Marie-Lou Dinet[3], Zakaria Jalal[3], Francois Laurent[1,2], Michel Montaudon[1,2], and Jean-Benoît Thambo[1,3]

[1]Department of Cardiovascular Imaging, Hôpital Cardiologique du Haut-Lévêque, CHU de Bordeaux, Avenue de Magellan, 33604 Pessac, France; [2]Department of Healthcare Technologies, IHU LIRYC, Université de Bordeaux—Inserm, Avenue du Haut Lévêque, 33604, Pessac, France; and [3]Department of Pediatric and Adult Congenital Cardiology, Hôpital Cardiologique du Haut-Lévêque, CHU de Bordeaux, Avenue de Magellan, 33604, Pessac, France

Received 13 November 2018; editorial decision 18 March 2019; accepted 26 March 2019; online publish-ahead-of-print 16 April 2019

Aims To identify the correlates of focal scar and diffuse fibrosis in patients with history of tetralogy of Fallot (TOF) repair.

Methods and results Consecutive patients with prior TOF repair underwent electrocardiogram, 24-h Holter, transthoracic echocardiography, exercise testing, and cardiac magnetic resonance (CMR) including cine imaging to assess ventricular volumes and ejection fraction, T1 mapping to assess left ventricular (LV) and right ventricular (RV) diffuse fibrosis, and free-breathing late gadolinium-enhanced imaging to quantify scar area at high spatial resolution. Structural imaging data were related to clinical characteristics and functional imaging markers. Cine and T1 mapping results were compared with 40 age- and sex-matched controls. One hundred and three patients were enrolled (age 28 ± 15 years, 36% women), including 36 with prior pulmonary valve replacement (PVR). Compared with controls, TOF showed lower LV ejection fraction (LVEF) and RV ejection fraction (RVEF), and higher RV volume, RV wall thickness, and native T1 and extracellular volume values on both ventricles. In TOF, scar area related to LVEF and RVEF, while LV and RV native T1 related to RV dilatation. On multivariable analysis, scar area and LV native T1 were independent correlates of ventricular arrhythmia, while RVEF was not. Patients with history of PVR showed larger scars on RV outflow tract but shorter LV and RV native T1.

Conclusion Focal scar and biventricular diffuse fibrosis can be characterized on CMR after TOF repair. Scar size relates to systolic dysfunction, and diffuse fibrosis to RV dilatation. Both independently relate to ventricular arrhythmias. The finding of shorter T1 after PVR suggests that diffuse fibrosis may reverse with therapy.

Keywords tetralogy of Fallot • cardiac magnetic resonance • late gadolinium-enhanced imaging • T1 mapping • myocardial fibrosis

Introduction

Over the past decades, advances in the surgical management of tetralogy of Fallot (TOF) have significantly improved survival, and the population of adults with repaired TOF (rTOF) is expanding.[1] However, patients frequently develop haemodynamic or electrophysiological disorders, leading to a rise in morbidity/mortality over the third/fourth decades of life.[2–4] These issues can be addressed with specific interventions, i.e. pulmonary valve replacement (PVR),[5] catheter ablation, or device implantation.[6] However, the mechanisms

* Corresponding author. Tel: +33 (5) 57656542; Fax: +33 (5) 57656509. E-mail: hcochet@wanadoo.fr

† The first two authors contributed equally to the study.

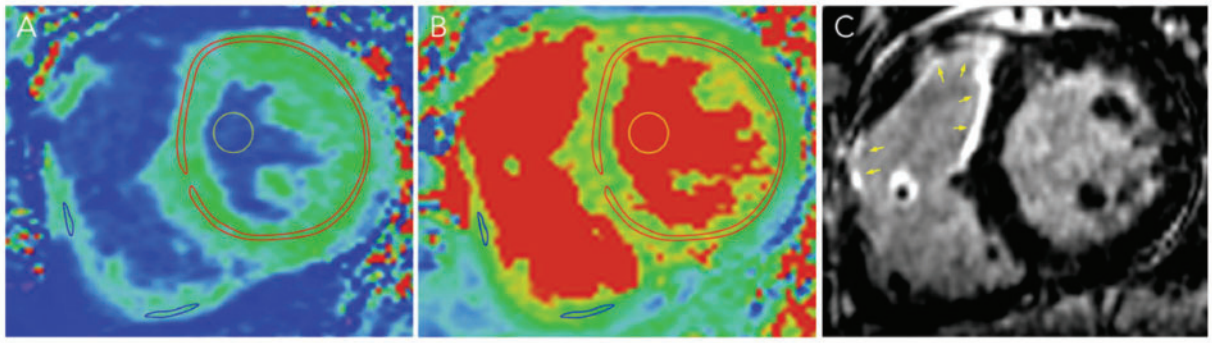

Figure 1 T1 measurements on the LV and RV. Identical regions of interest were drawn on native (*A*) and post-contrast (*B*) T1 maps. LV T1 was computed by averaging two regions drawn within the mid-wall layer on basal and mid-ventricular maps (red contours in *A* and *B*). RV T1 was computed by averaging a minimum of four regions drawn on basal and mid-ventricular maps (blue contours in *A* and *B*), RV measurements being only performed in areas with wall thickness >2.8 mm (two pixels). For both LV and RV regions, care was taken not to include areas exhibiting scar on LGE images (yellow arrows in *C*). Pre- and post-contrast T1 measurements were also performed within the blood pool (yellow contours in *A* and *B*) to enable the computation of ECV.[10]

involved in disease progression are still poorly understood, and the selection of candidates to undergo therapy remains challenging. In this prospect, the use of cardiac magnetic resonance (CMR) has expanded, given its ability to assess ventricular dilatation, systolic impairment, and pulmonary valve (PV) dysfunction.[7] Recent advances in CMR tissue characterization have provided new insights into remodelling mechanisms. T1 mapping was used to document the presence of diffuse fibrosis on both ventricles in rTOF.[8–12] Although no longitudinal study is yet available, CMR markers of diffuse fibrosis may become promising predictors of clinical outcome, and particularly arrhythmias.[10] On the other hand, late gadolinium-enhanced (LGE) imaging can be used to characterize focal scars,[13] which were shown associated with systolic dysfunction, exercise intolerance, and arrhythmia.[14] However, prior studies used 2D LGE methods whose spatial resolution (>6 mm thickness) may be insufficient to accurately characterize scars on the thin right ventricular (RV) wall, and scar burden was only estimated using semi-quantitative methods (segmental scores). In addition, the adverse effects of focal scars according to their anatomical location have not been thoroughly studied. The recent development of free-breathing LGE techniques has enabled dramatic improvements of spatial resolution.[15] These methods, initially developed for atrial imaging, were shown feasible for the detection and absolute quantification of focal scars in rTOF.[16] However, the correlates of such refined scar characterization have not been studied. This study aimed at identifying correlates of focal scar and diffuse fibrosis in rTOF by combining high-resolution LGE imaging and T1 mapping.

Methods

Population and non-CMR assessment

From May 2015 to June 2017, we enrolled consecutive patients with history of rTOF referred at the University Hospital of Bordeaux. Inclusion criteria comprised history of TOF with available information on the initial diagnosis and the surgical repair. Patients with subsequent history of PVR were eligible for inclusion if the time since PVR was >2 years. Exclusion criteria comprised contra-indications of CMR and inability to undergo CMR without general anaesthesia. Within a 48-h hospitalization, patients underwent electrocardiogram (ECG), 24-h Holter, transthoracic echocardiography (TTE), exercise testing, and CMR. CMR studies included cine imaging, velocity-encoded imaging, T1 mapping, and high-resolution LGE imaging starting from January 2016. CMR markers of diffuse fibrosis, focal scar burden, and focal scar distribution were compared with clinical and functional characteristics. In addition, cine and T1 mapping from 40 patients were compared with 40 age- and sex-matched controls. The control population was composed of patients with family history of arrhythmogenic cardiomyopathy or hypertrophic cardiomyopathy whose diagnostic work-up ended up negative ($N = 22$), and patients followed-up for dilated ascending aorta, with no valve dysfunction nor evidence of structural heart disease ($N = 18$). The study was approved by the institutional ethics committee, and all participants provided informed consent.

Non-CMR data

Clinical characteristics included demographics, age at repair, type of surgery, history of subsequent PVR, history of arrhythmia, and clinical symptoms. ECG was performed to measure QRS duration, and 24-h Holter ECG to document arrhythmia. Ventricular arrhythmia was defined by past history or 24-h Holter ECG evidence of frequent premature ventricular complexes (>500/24 h), non-sustained ventricular tachycardia (VT) (<30 s), sustained VT (>30 s), or ventricular fibrillation (VF)/aborted sudden death. Atrial arrhythmia was defined by past or present ECG evidence of supra-VT, atrial flutter, or atrial fibrillation. TTE was performed to look for PV dysfunction, PV stenosis/pressure overload being defined as maximum transpulmonary velocity >2 m/s, and PV regurgitation being considered significant when graded as moderate to severe. Cardiopulmonary exercise tests were conducted on a bicycle ergometer to document maximum exercise capacity.

CMR acquisition

CMR studies were conducted on a 1.5-T system (MAGNETOM Avanto, Siemens Healthineers, Erlangen, Germany) equipped with a 32-channel cardiac coil. Cine imaging was applied in two stacks of contiguous slices

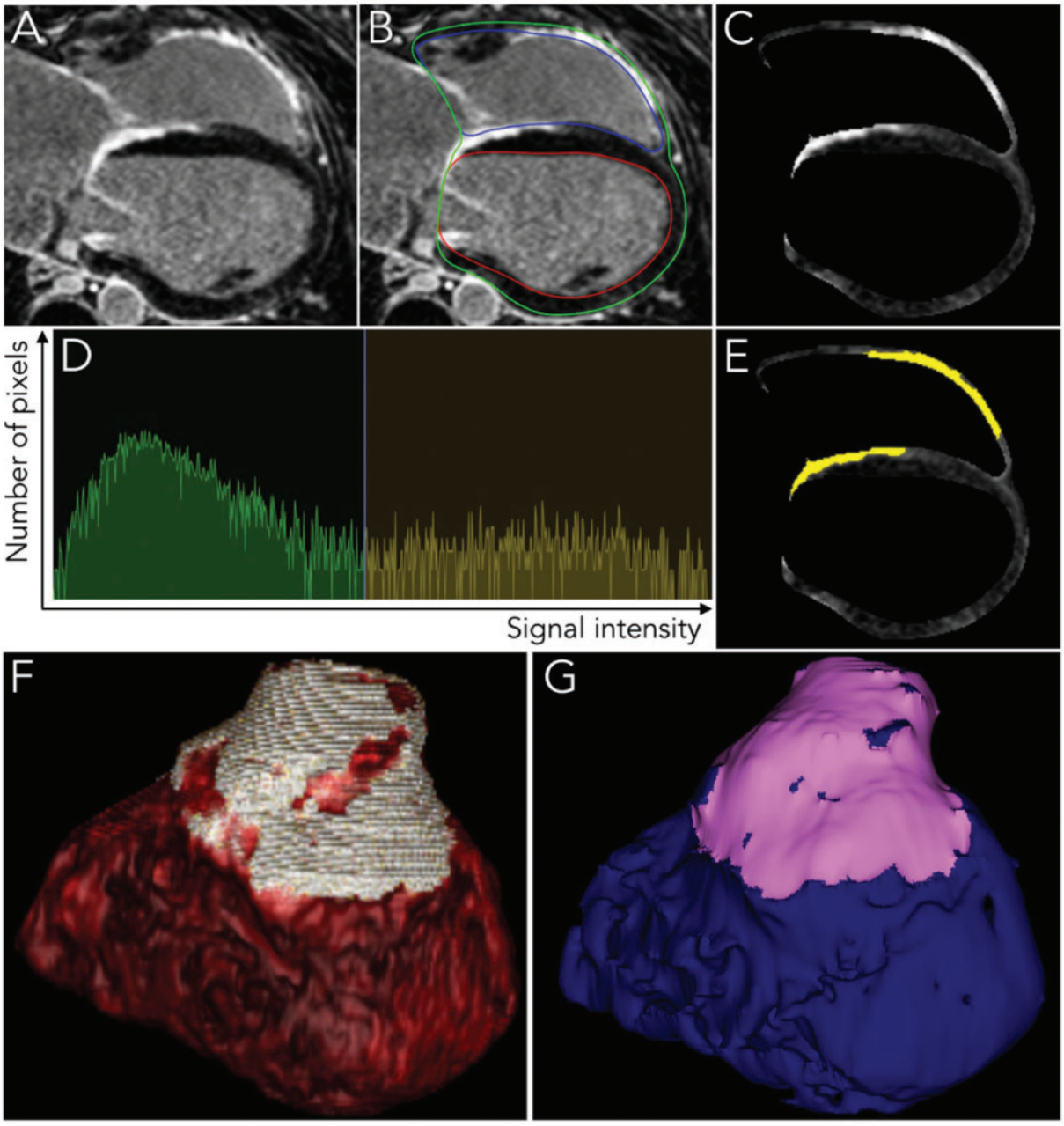

Figure 2 Quantification of scar area from high-resolution LGE images in patients with rTOF. On LGE images acquired during free breathing at high spatial resolution (*A*), endo- and epicardial contours were drawn (*B*) to segment the biventricular myocardium (*C*). The histogram of signal intensities in the myocardium was analysed (*D*), the scar threshold being set 3 SD above the mean intensity of the normal myocardium. This resulted in automated segmentation of scars within the myocardium (yellow region in *E*). Scar distribution was displayed on volume rendering reconstructions (*F*), and projected on an endocardial surface mesh (*G*) to automatically compute scar area.

encompassing both ventricles in short-axis and transaxial orientations, as well as in two perpendicular views aligned along the RV outflow tract (RVOT). Velocity-encoded imaging was performed in a plane perpendicular to the pulmonary artery positioned 1 cm above the PV. T1 mapping was performed in two short-axis views positioned at basal and mid-ventricular levels. Both native and post-contrast T1 mapping were performed, the latter being acquired 15 min after the injection of 0.2 mmol/kg gadoterate meglumine (Guerbet, Aulnay-sous-Bois, France). High-resolution LGE imaging was performed immediately after post-contrast T1 mapping, hence initiated approximately 17 min after injection, using a 3D, inversion-recovery-prepared, ECG-gated, respiration-navigated gradient-echo pulse sequence with fat-saturation.[14] Detailed sequence characteristics and parameters can be found in Supplementary data online, *Appendix*.

Table 1 Characteristics of patients with repaired TOF (*N* = 103)

Demographics	
Age (years)	28 ± 15
Female gender	37 (36%)
Clinical history	
Age at repair (months)	24 (11–45)
Type of repair	
VSD patch	103 (100%)
Transannular patch	75 (73%)
Sub-valvular patch or infundibulectomy	18 (17%)
RV-PA conduit	3 (3%)
No surgery on RVOT	7 (7%)
History of PVR	36 (35%)
Age at PVR (years)	22 ± 9
History of arrhythmia	24 (23%)
Frequent PVCs	10 (10%)
Non-sustained VT	6 (6%)
Sustained VT/VF	5 (5%)
Supra-ventricular tachycardia	5 (5%)
Atrial flutter	5 (5%)
Atrial fibrillation	2 (2%)
Clinical symptoms	
NYHA functional class	1.5 ± 0.6
Symptoms of RV failure	3 (3%)
Palpitations	31 (30%)
Light headedness	24 (23%)
Syncope	8 (8%)
Chest pain	21 (20%)
Maximum exercise capacity (W)	113 ± 37
ECG	
QRS duration (ms)	145 ± 24
TTE	
Pressure overload	42 (41%)
PV regurgitation	62 (60%)
CMR	
Cine MR	
LVEDV (mL/m^2)	78 ± 18
LVEF (%)	57 ± 9
RVEDV (mL/m^2)	124 ± 36
RVEF (%)	48 ± 11
RV wall thickness (mm)	3.4 ± 0.9
Velocity encoded MR	
PV regurgitation fraction (%)	32 (5–44)
PV regurgitation >20%	63 (61%)
T1 mapping	
LV native T1 (ms)	1002 ± 48
LV ECV (%)[a]	27.4 ± 3.3
RV T1 assessable	81 (79%)
RV native T1 (ms)	1023 ± 72
RV ECV (%)[b]	33.8 ± 4.5
LGE MR (*N* = 75)	
RVOT scar area (cm^2)	7 (4–9)
Septal scar area (cm^2)	4 (3–7)
Other scar on LV or RV	8 (11%)
Total scar area (cm^2)	11 (8–16)

Data are expressed as mean ± standard deviation when normally distributed, and median (interquartile range Q1–Q3) otherwise.
PVCs, premature ventricular complexes.
[a]Only in 50 (49%) patients with available haematocrit on the day of the CMR study.
[b]Only in 44 (43%) patients with assessable RV T1 and available haematocrit on the day of the CMR study.

CMR analysis

The processing of cine, velocity-encoded, and T1 mapping images was performed using Argus software (Siemens Healthineers, Erlangen, Germany) by an observer with 15-year experience in CMR. Ventricular end-diastolic volume, end-systolic volume, and ejection fraction were derived from short-axis images for the left ventricle, and transaxial images for the right ventricle. RV thickness was assessed on a mid-ventricular short-axis cine image at end-diastole, and computed by averaging four thickness measurements on lateral and inferior RV regions showing no LGE, excluding trabeculations. On velocity-encoded images, the pulmonary artery was contoured to compute PV regurgitation fraction, considered significant when >20%. T1 maps were automatically computed by using a commercially available elastic registration algorithm (MoCo technique, Siemens Healthineers, Erlangen, Germany). Manual measurements on the original series were performed in case of suboptimal registration. Identical regions of interest were drawn within the myocardium and the left ventricular (LV) blood pool on both pre-contrast and post-contrast T1 maps. On the left ventricle, T1 was averaged from two mid-myocardial regions positioned throughout the LV circumference on basal and mid-ventricular slices. On the right ventricle, T1 was only measured in areas with wall thickness >2.8 mm (two pixels), and averaged over a minimum of four measurements on RV lateral and inferior wall. For all T1 measurements, care was taken to exclude any area exhibiting LGE. The computation of extracellular volume (ECV) was only performed in case haematocrit level had been measured on the day of the CMR study. The measurement of RV and LV T1 is illustrated in *Figure 1*. The processing of high-resolution LGE images was performed using MUSIC software (IHU Liryc, University of Bordeaux and Inria Sophia Antipolis, France). In-plane and through-plane interpolation was applied to resample the imaging volume at the voxel size of 0.625 × 0.625 × 1 mm. Semi-automated tools were used to segment endocardial and epicardial contours of both ventricles. Iterative histogram thresholding was applied to segment myocardial scar, the threshold being set 3 SD above the mean intensity within the normal myocardium, as measured in a normal septal area. The endocardial segmentation was used to compute a 3D surface mesh at high density (>50 000 triangles), on which myocardial scars were projected and scar areas automatically measured. To characterize scar distribution, separate quantifications were made for RVOT scar, septal scar, and scar on other RV/LV locations. The quantification of scar from high-resolution LGE is illustrated in *Figure 2*.

Statistical analysis

The Shapiro–Wilk test of normality was used to assess whether quantitative data conformed to the normal distribution. Continuous data are expressed as mean ± standard deviation when following a normal distribution, and median (interquartile range Q1–Q3) otherwise. Categorical data are expressed as fraction (%). Independent continuous variables were compared using independent-sample parametric (unpaired

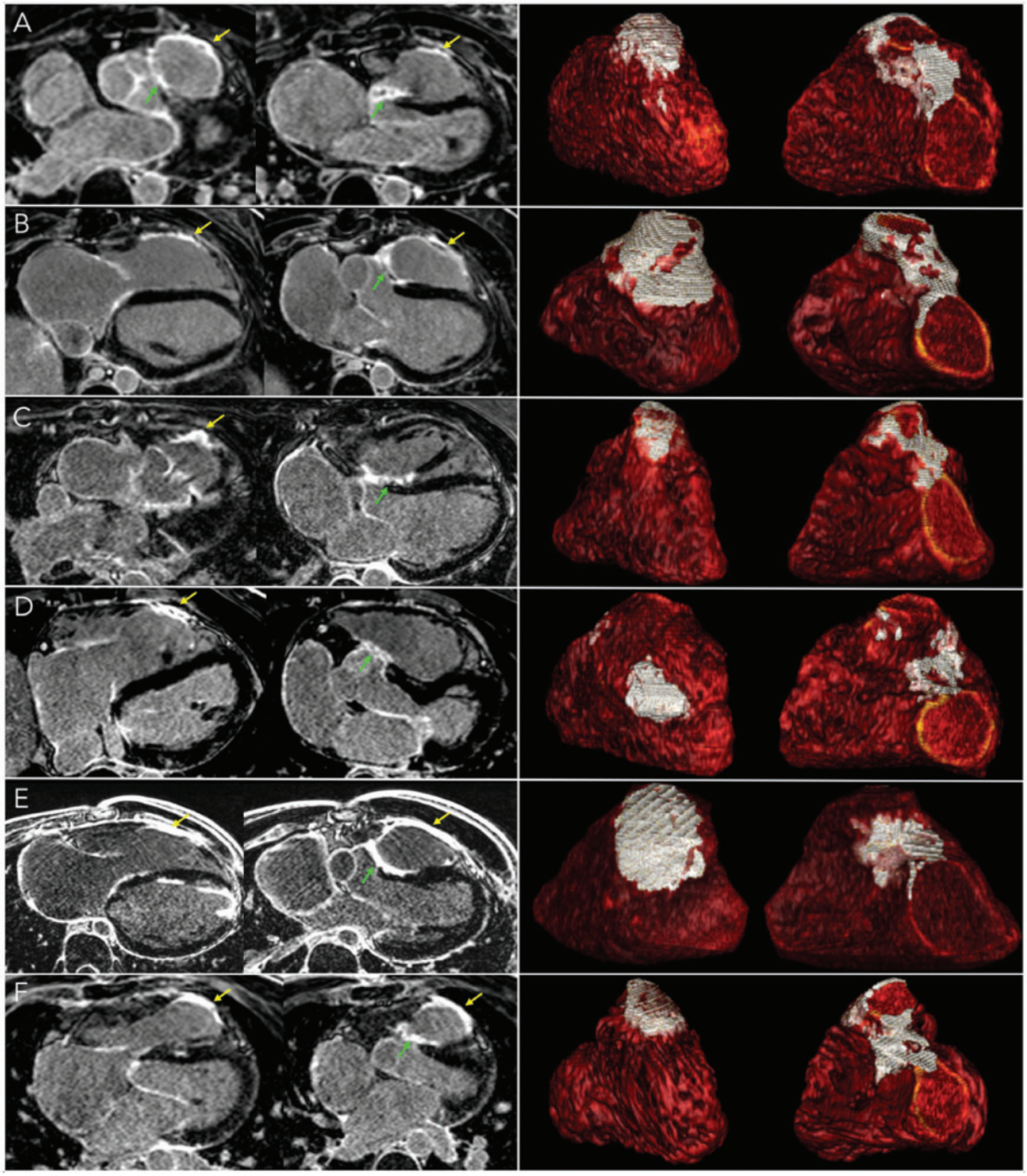

Figure 3 Examples of scar distributions on high-resolution LGE images in patients with rTOF. LGE data from six patients are shown (*A* through *F*). Trans-axial LGE images are shown in the left column, yellow and green arrows indicating RVOT and septal scars, respectively. In the right column, the corresponding scar distributions are displayed in RVOT and septal views (left and right images, respectively). (*A*) A 27-year-old man with RVOT scar (transannular patch) of average size (8 cm^2), and large septal scar (11 cm^2). (*B*) A 29-year-old man with large RVOT and septal scars (24 and 12 cm^2, respectively). (*C*) A 26-year-old woman with small scars on RVOT and septum (3 and 4 cm^2, respectively). (*D*) A 33-year-old man with infundibulectomy without patch (RVOT scar 4 cm^2) and septal scar of average size (5 cm^2). (*E*) A 25-year-old man with large RVOT scar (20 cm^2) and large septal scar (10 cm^2). (*F*) A 40-year-old woman with small RVOT scar (5 cm^2) and large septal scar (9 cm^2).

Table 2 CMR characteristics in TOF and matched controls

	TOF ($N = 40$)	Controls ($N = 40$)	*P*-value
Age (years)	26 ± 14	27 ± 14	0.87
Female gender	8 (20%)	8 (20%)	1
Cine MR			
LVEDV (mL/m^2)	79 ± 18	76 ± 12	0.23
LVESV (mL/m^2)	35 ± 16	29 ± 8	<0.001
LVEF (%)	56 ± 11	62 ± 8	<0.001
RVEDV (mL/m^2)	136 ± 49	76 ± 13	<0.001
RVESV (mL/m^2)	73 ± 30	38 ± 10	<0.001
RVEF (%)	48 ± 13	52 ± 9	0.02
RV wall thickness (mm)	3.5 ± 1.1	2.7 ± 0.8	<0.001
T1 mapping			
LV native T1 (ms)	1014 ± 51	975 ± 38	<0.001
LV ECV (%)[a]	27.2 ± 3.5	23.9 ± 2.0	<0.001
RV T1 assessable	36 (90%)	24 (60%)	0.001
RV native T1 (ms)[b]	1039 ± 67	937 ± 118	<0.001
RV ECV (%)[c]	34.0 ± 4.6	29.2 ± 4.2	0.002

[a]Only available in 32 (80%) TOF and 27 (68%) controls with haematocrit on the day of the CMR study.
[b]Only available in 36 (90%) TOF and 27 (68%) controls with assessable T1 on the RV.
[c]Only available in 28 (70%) TOF and 14 (35%) controls with available haematocrit and assessable T1 on the RV.

Student's *t*-test) or non-parametric tests (Mann–Whitney *U* test) depending on data normality. Dependent continuous variables were compared using paired-sample parametric or non-parametric tests (paired Student's *t*-test, Wilcoxon signed-rank test) depending on data normality. Independent categorical variables were compared using χ^2 test when expected frequencies were ≥5, and Fisher's exact test when these were <5. Relationships between continuous variables were assessed by computing Pearson or Spearman correlation coefficients, as appropriate. Relationships between categorical and continuous variables were assessed using the correlation ratio, defined as the square-root of between-groups sum of squares divided by the total sum of squares. Multivariable logistic regression analyses were used to identify independent correlates of ventricular arrhythmia. Assuming an expected prevalence of ventricular arrhythmia of about 17% based on prior publications,[10,14] the study was populated to enable the inclusion of three variables in multivariable models.[17] All statistical tests were two-tailed, and a *P*-value <0.05 was considered to indicate statistical significance. Analyses were performed using NCSS 8 (NCSS Statistical Software, Kaysville, UT, USA).

Results

Population characteristics

The characteristics of the studied population are provided in *Table 1*. One hundred and three patients were enrolled. Repair consisted of a patch covering the ventricular septal defect in all patients. On the RVOT, repair consisted of a transannular patch in the majority of patients (73%), a non-transannular patch or simple ventriculotomy in 17%, a RV pulmonary artery conduit in 3%. Seven patients (7%) had no history of surgery on RVOT. Thirty-six (35%) patients also underwent PVR. Prior history of arrhythmia was reported in 24 (23%) patients (atrial in 12%, ventricular in 20%). Results from TTE, cine and velocity-encoded CMR can be found in *Table 1*. Native T1 was assessable in all patients on the left ventricle, and in 79% on the right ventricle. Because haematocrit level was not consistently measured on the day of the CMR study, ECV values were only available in 49% patients on the left ventricle, and in 43% on the right ventricle. Free-breathing LGE was performed in 75 (73%) patients. In this population, RVOT scar was found in all 69 patients with history of RVOT surgery, and in none of the six patients with no prior RVOT surgery. Septal scar was found in all patients. Eight (11%) patients also showed scar on other locations (on the left ventricle in four, right ventricle in one, both ventricles in three). Examples of scar distributions on high-resolution LGE images are provided in *Figure 3*, and further illustrated in Supplementary data online, *Movies S1–S6*.

Reproducibility of CMR markers of focal scar and diffuse fibrosis

The reproducibility of CMR markers of focal scar and diffuse fibrosis was assessed on a subset of 30 patients randomly selected from the 56 patients with both LV and RV native T1 assessable, and available high-resolution LGE CMR data. Image processing was performed by two readers to quantify native T1 on both ventricles and total scar area, the agreement between the two measurements being assessed using intraclass correlation coefficients and Bland and Altman analyses. We found excellent reproducibility for scar area measurements, with an intraclass correlation coefficient of 0.97, a mean bias of +0.4 cm^2, and 95% limits of agreement from -4.5 to +5.2 cm^2. Reproducibility was also good for LV native T1 measurements, with an intraclass correlation coefficient of 0.95, a mean bias of +2 ms, and 95% limits of agreement from -34 to +38 ms. The reproducibility for RV native T1 measurements was substantially lower, with an intraclass correlation coefficient of 0.87, a mean bias of +4 ms, and 95% limits of agreement from -71 to +81 ms.

Comparison between TOF and controls

Cine and T1 mapping results in TOF and controls are compared in *Table 2*. Patients with rTOF showed lower LV ejection fraction (LVEF), lower RV ejection fraction (RVEF), and higher RV end-diastolic volume (RVEDV). RV native T1 was more often assessable in TOF than in controls because of thicker RV wall. TOF patients showed longer native T1 and higher ECV on both ventricles. In both TOF and controls, ECV values were higher on the right ventricle than on the left ventricle. Native T1 values also tended to be longer on the right ventricle, although the difference did not reach statistical significance.

Correlates of focal scar and diffuse fibrosis in TOF

Univariable correlates of RVEDV and RVEF are provided in Supplementary data online, *Table*. Univariable correlates of CMR

Table 3 Univariable correlates of focal scar and diffuse fibrosis

	Relationship with total scar (*N* = 75)		Relationship with LV native T1 (*N* = 103)	
	***R* value**	***P*-value**	***R* value**	***P*-value**
Demographics				
Age (years)	**0.28**	**0.01**	0.11	0.29
Female gender	0.07	0.53	0.14	0.16
Clinical history				
Age at repair (months)	**0.26**	**0.03**	**0.24**	**0.02**
History of PVR	**0.35**	**0.002**	**−0.29**	**0.003**
History of ventricular arrhythmia	**0.56**	**<0.001**	**0.35**	**<0.001**
History of atrial arrhythmia	0.20	0.08	**0.30**	**0.002**
Clinical symptoms				
NYHA functional class	0.04	0.74	**0.37**	**<0.001**
Maximum exercise capacity (W)	0.18	0.16	**−0.32**	**0.003**
ECG				
QRS duration (ms)	**0.29**	**0.01**	–0.04	0.68
TTE				
Pressure overload	0.21	0.07	–0.14	0.18
CMR				
Cine MR				
LVEDV (mL/m^2)	0.20	0.10	0.10	0.33
LVEF (%)	**−0.31**	**0.008**	–0.14	0.14
RVEDV (mL/m^2)	0.15	0.21	**0.43**	**<0.001**
RVEF (%)	**−0.42**	**<0.001**	0.02	0.85
RV wall thickness (mm)	**0.24**	**0.04**	–0.06	0.57
Velocity encoded MR				
PV regurgitation fraction (%)	0.02	0.88	**0.29**	**0.003**
T1 mapping				
LV native T1 (ms)	0.12	0.30	NA	NA
RV native T1 (ms)[a]	0.13	0.35	**0.68**	**<0.001**
LGE MR (*N* = 75)				
RVOT scar area (cm^2)	NA	NA	0.04	0.76
Septal scar area (cm^2)	NA	NA	0.08	0.48
Scar on other LV/RV locations	NA	NA	0.17	0.14
Total scar area (cm^2)	NA	NA	0.12	0.30

Boldface values indicate statistical significance.
[a]RV T1 correlations with total scar and LV T1 were assessable on 56 and 81 patients, respectively.

markers of focal scar and diffuse fibrosis are provided in *Table 3*. Good correlation was found between RV and LV native T1 values, as illustrated in *Figure 4*. No significant association was found between the extent of focal scar and CMR markers of diffuse fibrosis. Total scar area inversely related to RVEF and LVEF, and positively related to age, age at repair, history of ventricular arrhythmia, history of PVR, and QRS duration. LV native T1 inversely related to history of PVR and maximum capacity on exercise testing, and positively related to age at repair, history of ventricular arrhythmia, atrial arrhythmia, New York Heart Association (NYHA) functional class, RVEDV, and PV regurgitation fraction. The association of CMR markers of focal scar and diffuse fibrosis with RV dilatation and systolic dysfunction is illustrated in *Figure 5*. The association of LV native T1 with NYHA functional class and maximum exercise capacity is illustrated in *Figure 6*.

Characteristics of patients with history of PVR

The characteristics of patients with (*N* = 36) and without (*N* = 67) prior PVR are compared in *Table 4*. Patients with history of PVR obviously showed lower PV regurgitation fraction and RVEDV. They also showed lower RVEF, LVEF and thicker RV wall on cine CMR, as well as larger scars on LGE CMR (particularly on RVOT), and interestingly shorter native T1 on both ventricles.

Characteristics of patients with history of ventricular arrhythmia

The characteristics of patients with (*N* = 21) and without (*N* = 82) history of ventricular arrhythmia are compared in *Table 5*. Patients

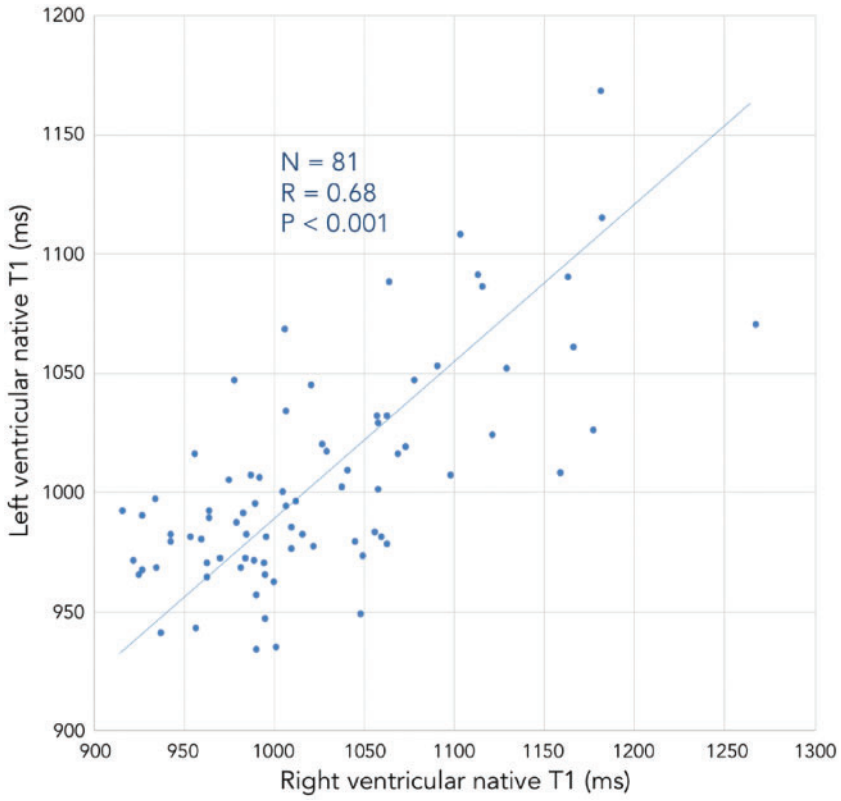

Figure 4 Relationship between left and right ventricular native T1 measurements.

with prior ventricular arrhythmia were older and were more likely to also present with atrial arrhythmia. They also showed lower RVEF, lower LVEF, and higher LV end-diastolic volume on cine CMR, and longer native T1 on both ventricles. On LGE imaging, they showed much larger scars particularly on the septum and were more likely to have scars on LV/RV locations other than RVOT and septum. Multivariable correlates of ventricular arrhythmia are analysed in *Table 6*. When combining RVEF, LV native T1 and total scar area in a multivariable regression model, total scar area and LV native T1 remained strongly and independently related to ventricular arrhythmia, while RVEF did not. Scar area, LV native T1, and RVEF values in patients with vs. without history of ventricular arrhythmia are shown in *Figure 7*. Among patients with ventricular arrhythmias, five showed either sustained VT or VF/aborted sudden death. When compared with the rest of the population, these showed markedly higher scar area [median 38.0 (Q1–Q3: 34.8–45.3) vs. 11.2 (7.4–14.4) cm^2, $P < 0.001$] and lower RVEF [31 (25–41) vs. 47 (42–54) %, $P = 0.01$]. They also showed higher LV native T1 values although the difference did not reach statistical significance [1034 (1007–1088) vs. 992 (972–1023) ms, $P = 0.06$].

Discussion

This study is to our knowledge the first analysing the correlates of focal scar and diffuse fibrosis in rTOF using a quantitative approach based on state-of-the-art T1 mapping and high-resolution LGE imaging. Its main findings are that (i) focal scar and diffuse fibrosis in rTOF are independent markers, (ii) focal scar relates to biventricular systolic dysfunction, while diffuse fibrosis relates to RV dilatation, (iii) focal scar and diffuse fibrosis are independent correlates of ventricular arrhythmia, and (iv) patients with prior PV replacement have larger scars on RVOT but lower markers of diffuse fibrosis, suggesting that the latter may reverse with therapy.

Population and methods

The population characteristics are consistent with past large series of rTOF. One discrepancy with prior reports on young adults with rTOF may be the quite high prevalence of ventricular arrhythmia (20%), which is likely due to a referral bias, our site being a tertiary centre for the management of arrhythmias. On CMR, the characteristics of the studied population are similar to prior CMR studies in rTOF in terms of ventricular volume, systolic dysfunction, and degree of PV regurgitation.[10] Regarding CMR markers of diffuse fibrosis, a series of prior studies have reported evidence of biventricular fibrosis in rTOF,[8–12] RV fibrosis being observed quite early in the course of the disease.[11,12] Our results are in line with these studies, indicating increased burden of diffuse fibrosis on both ventricles in adult patients with rTOF when compared with controls. We found longer T1 and higher ECV values than in most studies. This is likely due to patient age, our ECV values being consistent with a report by Broberg *et al.*[18] in adult patients with rTOF. Discrepancies in T1 measurements may also be explained by the variability of measures

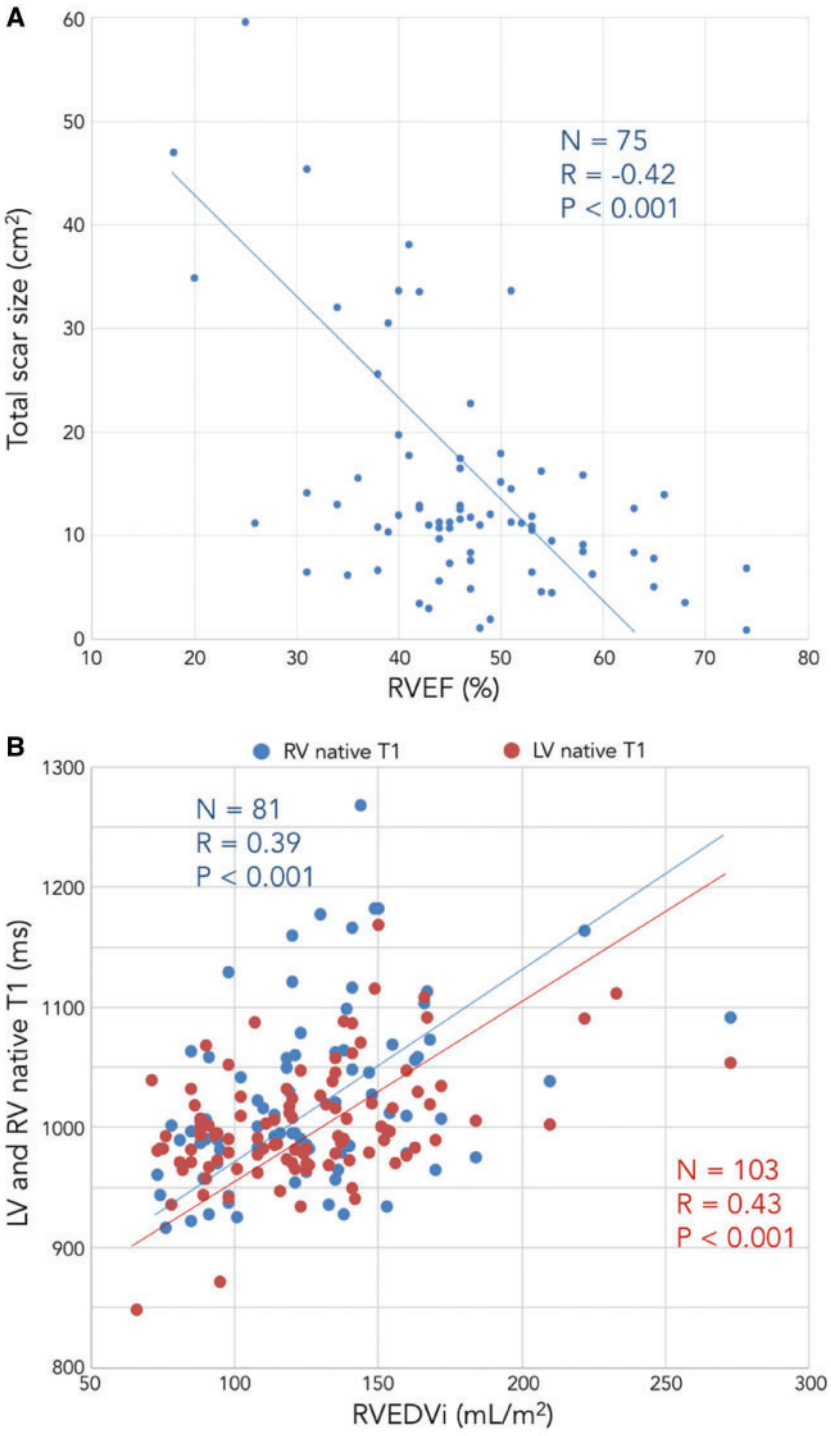

Figure 5 Relationship between CMR tissue characteristics and right ventricular dilatation and systolic dysfunction in rTOF.

between magnetic resonance imaging scanners.[19] Regarding focal scar, prior studies showed that conventional breath-held LGE methods can detect focal scars within the RV wall after TOF repair, despite limited spatial resolution (slice thickness >6 mm).[13,14,20] The scar quantification reported in the present study cannot be compared with existing literature, because the imaging methods used in prior studies only allowed for semi-quantitative assessment of scar burden based on segmental scores. One prior study had demonstrated the feasibility of acquiring free-breathing LGE images at high spatial resolution in rTOF.[16] In the present work, we have applied a similar acquisition method, although we chose to quantify scar surface rather than scar volume to maximize reproducibility. As expected septal scar is

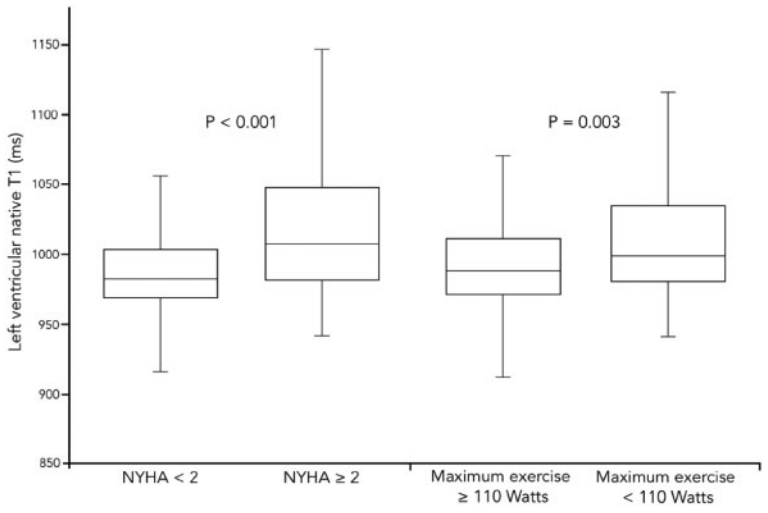

Figure 6 Association of LV native T1 with NYHA functional class and maximum exercise capacity in patients with rTOF.

Table 4 Characteristics of TOF patients with vs. without history of PV replacement

	History of PVR (*N* = 18)	No history of PVR (*N* = 46)	*P*-value
Demographics			
Age (years)	27 ± 13	25 ± 15	0.50
Female gender	5 (28%)	14 (30%)	0.84
Clinical history			
Age at repair (months)	22 (12–38)	17 (9–36)	0.70
History of atrial arrhythmia	2 (11%)	8 (17%)	0.61
History of ventricular arrhythmia	6 (33%)	10 (22%)	0.34
Clinical symptoms			
NYHA functional class	1.5 ± 0.8	1.6 ± 0.6	0.79
Maximum exercise capacity (W)	113 ± 34	111 ± 35	0.84
ECG			
QRS duration (ms)	144 ± 28	139 ± 26	0.55
TTE			
PV stenosis	10 (56%)	23 (50%)	0.44
CMR			
Cine MR (*N* = 64)			
LVEDV (mL/m^2)	74 ± 15	78 ± 17	0.36
LVEF (%)	56 ± 11	59 ± 9	0.32
RVEDV (mL/m^2)	107 ± 26	140 ± 39	**0.002**
RVEF (%)	43 ± 15	51 ± 9	**0.01**
RV wall thickness (mm)	4.0 ± 1.0	3.5 ± 1.0	0.05
Velocity encoded MR (*N* = 64)			
PV regurgitation fraction (%)	0 (0–7.5)	40 (29–48)	**<0.001**
T1 mapping (*N* = 64)			
LV native T1 (ms)	993 ± 49	1022 ± 51	**0.04**
RV native T1 (ms)[a]	996 ± 46	1053 ± 83	**0.01**
LGE MR (*N* = 40)			
RVOT scar area (cm^2)	11 (7–15)	6 (3–9)	**0.02**
Septal scar area (cm^2)	5 (4–9)	4 (3–8)	0.72
Other scar on LV or RV	2 (11%)	3 (7%)	0.42
Total scar area (cm^2)	16 (13–32)	11 (8–16)	**0.03**

Data are expressed as mean ± standard deviation when normally distributed, and median (interquartile range Q1–Q3) otherwise.
Boldface values indicate statistical significance.
[a]Only available in 17 patients with prior PVR and 41 patients with no prior PVR.

Table 5 Characteristics of TOF patients with vs. without ventricular arrhythmia

	Ventricular arrhythmia (*N* = 21)	No ventricular arrhythmia (*N* = 82)	*P*-value
Demographics			
Age (years)	34 ± 13	26 ± 15	**0.004**
Female gender	10 (48%)	27 (33%)	0.21
Clinical history			
Age at repair (months)	36 (20–48)	18 (11–42)	0.06
History of PVR	10 (48%)	26 (32%)	0.17
History of atrial arrhythmia	9 (43%)	3 (4%)	**<0.001**
Clinical symptoms			
NYHA functional class	1.7 ± 0.7	1.5 ± 0.6	0.19
Maximum exercise capacity (W)	108 ± 33	114 ± 38	0.50
ECG			
QRS duration (ms)	152 ± 33	143 ± 22	0.25
TTE			
Pressure overload	8 (38%)	34 (41%)	0.77
CMR			
Cine MR			
LVEDV (mL/m^2)	86 ± 19	76 ± 17	**0.02**
LVEF (%)	51 ± 14	59 ± 7	**0.02**
RVEDV (mL/m^2)	137 ± 40	121 ± 34	0.08
RVEF (%)	42 ± 11	49 ± 10	**0.002**
RV wall thickness (mm)	3.5 ± 1.1	3.4 ± 0.9	0.60
Velocity encoded MR			
PV regurgitation fraction (%)	30 (2–42)	32 (9–44)	0.75
T1 mapping			
LV native T1 (ms)	1038 ± 55	993 ± 42	**<0.001**
RV native T1 (ms)[a]	1075 ± 74	1011 ± 66	**<0.001**
LGE MR (*N* = 75)[b]			
RVOT scar area (cm^2)	11 (6–20)	6 (4–8)	**0.01**
Septal scar area (cm^2)	11 (7–14)	4 (3–5)	**<0.001**
Other scar on LV or RV	7 (44%)	1 (2%)	**<0.001**
Total scar area (cm^2)	27 (16–36)	11 (7–13)	**<0.001**

Data are expressed as mean ± standard deviation when normally distributed, and median (interquartile range Q1–Q3) otherwise.
Boldface values indicate statistical significance.
[a]RV T1 values only available in 16 patients with ventricular arrhythmia and 65 patients with no ventricular arrhythmia.
[b]LGE MR data only available in 16 patients with ventricular arrhythmia and 59 patients with no ventricular arrhythmia.

found in all patients with rTOF in the area of the patch covering the ventricular septal defect. Interestingly, the size of septal scars is highly variable between patients (range 1–22 cm^2 in our series), possibly reflecting both the size of the initial defect, and potential subsequent mechanically or ischaemia-induced remodelling of the tissue adjacent to the patch over the course of the disease. The size of scars on the RVOT is also quite variable, as expected, given the variety of surgical techniques applied in this region. Last, focal scars on other anatomical locations are also quite common (11% in our series), which is in line with prior studies.[14]

Correlates of focal scar and diffuse fibrosis

Applying segmental scoring to assess scar burden on conventional LGE images, several authors reported promising correlates, including association with systolic dysfunction, exercise intolerance, and arrhythmia.[14,20] However, the spatial resolution of such methods may be insufficient to accurately characterize the RV wall, and the robustness of semi-quantitative approaches may be sub-optimal. Of note, recent data suggests that segmental scar scores derived from conventional LGE imaging are weaker predictors of arrhythmia than clinical status and ventricular dilatation.[20] Using a quantitative approach on images of higher spatial resolution, our results indicate that scar burden is a major determinant of LV and RV systolic dysfunction, closely related to ventricular arrhythmia, and to the degree of electrical dyssynchrony. In contrast, CMR markers of diffuse fibrosis do not seem to be influenced by focal scar burden, and show different functional correlates, rather related to RV dilatation and to the degree of PV regurgitation than to systolic dysfunction, which is in line with prior reports.[8,10,12] These discrepancies suggest that CMR markers of focal

Table 6 Multivariable correlates of ventricular arrhythmia

	R^2 value	*P*-value
Two-variable model		
Total scar area, RVEF		
Total scar area	0.376	<0.001
RVEF	0.003	0.64
Model's R^2	0.379	
Two-variable model		
LV native T1, RVEF		
LV native T1	0.145	<0.001
RVEF	0.130	0.001
Model's R^2	0.275	
Two-variable model		
Total scar area, LV native T1		
Total scar area	0.376	<0.001
LV native T1	0.150	0.004
Model's R^2	0.526	
Three-variable model		
Total scar area, LV native T1, RVEF		
Total scar area	0.376	0.003
LV native T1	0.150	0.003
RVEF	0.021	0.23
Model's R^2	0.547	

scar and diffuse fibrosis burden may have independent prognostic value. Interestingly, both are strongly and independently related to ventricular arrhythmia. This may explain why focal scars that are present since the early years of life only become arrhythmogenic decades after surgery, due to progressive diffuse interstitial remodelling of the adjacent myocardial tissue over the course of the disease. Of note, rhythmic disorders more closely relate to scar on the septum and at other LV and RV locations than to scar on the RVOT. This may be due to the high prevalence of transannular patches, which may be less arrhythmogenic. Indeed, the mechanism leading to re-entrant tachycardia in rTOF is known to be related to anatomical isthmuses of viable myocardium interposed between the patches and the PV and tricuspid annuli.[21] These areas of slow conduction are quite frequent in the vicinity of the septal patch, but much less on the RVOT when a transannular patch acts as a complete conduction block. Interestingly, we found both the scar size and the degree of diffuse fibrosis to be associated with an older age at repair, which may explain the poorer outcomes usually reported in this population.[2] Of note, our results confirm that LV and RV T1 values are closely related, and share the same correlates. This finding is in line with prior reports,[10] and suggests that interstitial remodelling in rTOF is induced by diffuse signalling pathways involving both the right and left ventricles, possibly due to coupling mechanisms such as abnormal septal motion and ventricular dyssynchrony. This ventricular interdependence has been documented by other authors in rTOF as well as in other congenital or acquired heart diseases.[22,23] Regarding clinical status, we found LV native T1 to be the best imaging correlate of NYHA functional class, and a significant predictor of exercise intolerance. These findings support research on specific therapies targeting interstitial fibrosis in patients with rTOF,[24] firstly because fibrosis may be reversible (as opposed to focal scars), and secondly because it may both improve current clinical status and reduce future occurrence of arrhythmia.

Characteristics of patients with PV replacement

In this study, we chose not to exclude patients with history of prior PVR. Indeed, PVR is extremely common in adults with rTOF, and although its impact on ventricular and PV function is well documented,[25] its impact on focal scars and diffuse fibrosis remains unknown. We acknowledge that this topic should ideally be addressed in a longitudinal fashion, but in our opinion our results open promising perspectives. As expected, patients with PVR have lower RV volumes and PV regurgitation. But these also show increased scar burden on RVOT, which is likely the consequence of the additional surgery performed in the area. Moreover, we found native T1 to be markedly lower in patients with PVR on both ventricles. This suggests that diffuse fibrosis may reverse after therapy, a finding that opens interesting perspectives for the management of patients with rTOF.

Study limitations

The main limitation of this study is the absence of follow-up to prospectively assess outcome. Although strong associations were found between imaging markers and clinical characteristics, these cannot be interpreted as predictors. Another limitation is related to the potential underestimation of asymptomatic arrhythmic episodes. We addressed this issue by performing 24-h Holter ECG in all patients but we acknowledge that this may have altered our results. Regarding the definition used for ventricular arrhythmias, we acknowledge that it includes events of variable clinical significance, and that using only sustained VT and VF/aborted sudden death would be a harder endpoint. However, given the relatively low prevalence of sustained arrhythmia in young adults with rTOF,[2] this would have required a cohort of hundreds of patients. In addition, the finding of non-sustained VT or frequent premature ventricular complexes on 24-h Holter recordings were shown to be related to a higher risk of sudden cardiac death in rTOF.[26,27] We also acknowledge that the spatial resolution of T1 maps may be insufficient to study the RV wall, and that differences between LV and RV native T1 and ECV values may be due to partial volume effect. However, all RV measurements were performed on sites of sufficient wall thickness to minimize partial volume effect, good correlation was found between RV and LV T1 values, significant differences were found with RV measurements performed in controls, and the correlates of RV native T1 in patients with rTOF are consistent with prior reports.[10–12] Nonetheless, given that RV T1 measurements have lower feasibility and reproducibility, and provide similar information as LV T1 measurements, one may question the clinical value of measuring T1 on the right ventricle. In addition, because T1 can only be measured in thicker RV areas, one may question whether this is representative of the entire RV myocardium. Another limitation is the use of maximal exercise workload instead of peak oxygen uptake to document exercise intolerance. We acknowledge that using VO_2 max would have been more rigorous,

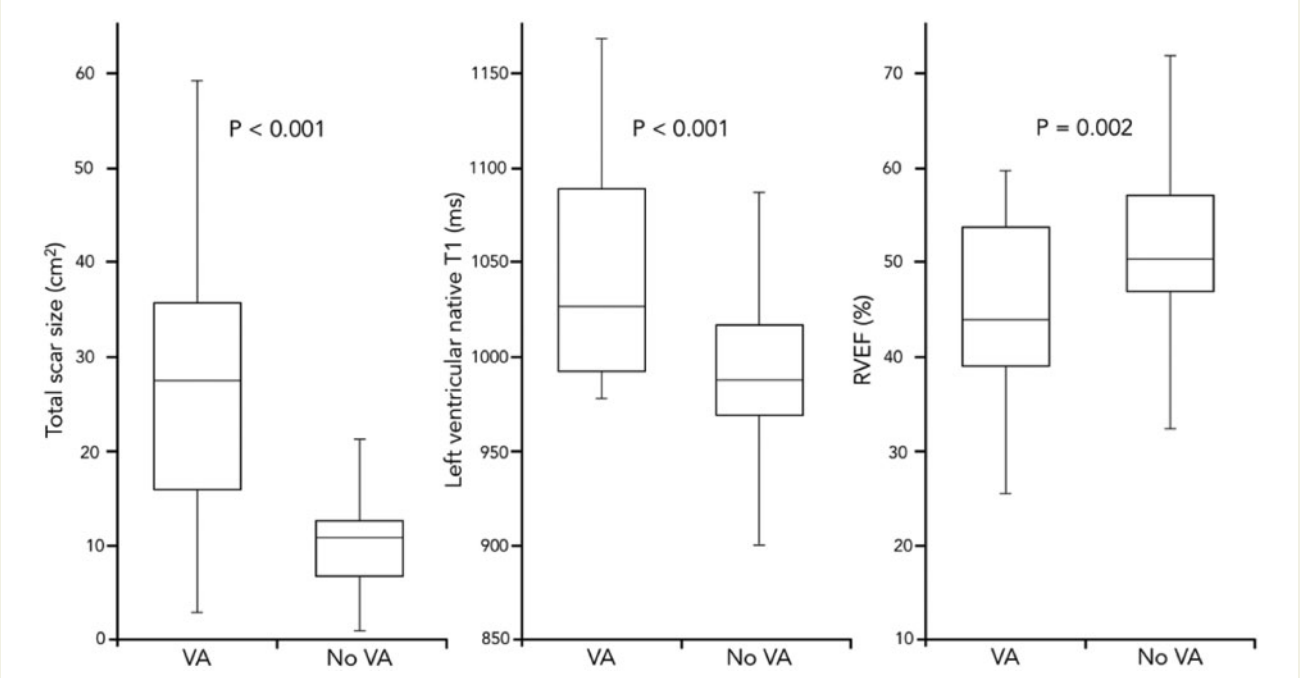

Figure 7 Scar area, LV native T1, and RVEF values in patients with vs. without history of ventricular arrhythmia.

but this data was unfortunately not available in our entire study population, exercise testing being mainly performed in our patients to look for exercise-induced arrhythmias. Last, this study focused on focal scar and diffuse fibrosis, and several promising imaging markers were not studied, such as RV pressure[28] or tricuspid regurgitation[29] on TTE, and regional myocardial motion or deformation on CMR.[30,31]

Conclusions

Focal scars and diffuse fibrosis are common in patients with rTOF and can be readily quantified with the use of CMR. These are independent markers, focal scar area relating to biventricular systolic dysfunction, while diffuse fibrosis relates to RV dilatation. Scar area and the degree of diffuse fibrosis are independent correlates of ventricular arrhythmia. Patients with prior PV replacement have larger scar on RVOT but lower markers of diffuse fibrosis, suggesting that the latter may reverse with therapy.

Supplementary data

Supplementary data are available at *European Heart Journal - Cardiovascular Imaging* online.

Funding

The research leading to these results has received funding from l'Agence Nationale de la Recherche (ANR) under Grant Agreements ANR-11-EQPX-0030 and ANR-10-IAHU-04, and from the European Research Council under Grant Agreement ERC n°715093.

Conflict of interest: none declared.

References

1. Marelli AJ, Ionescu-Ittu R, Mackie AS, Guo L, Dendukuri N, Kaouache M. Lifetime prevalence of congenital heart disease in the general population from 2000 to 2010. *Circulation* 2014;**130**:749–56.
2. Gatzoulis MA, Balaji S, Webber SA, Siu SC, Hokanson JS, Poile C *et al.* Risk factors for arrhythmia and sudden cardiac death late after repair of Tetralogy of Fallot: a multicentre study. *Lancet* 2000;**356**:975–81.
3. Chiu SN, Wang JK, Chen HC, Lin MT, Wu ET, Chen CA *et al.* Long-term survival and unnatural deaths of patients with repaired tetralogy of Fallot in an Asian cohort. *Circ Cardiovasc Qual Outcomes* 2012;**5**:120–5.
4. Cuypers JA, Menting ME, Konings EE, Opić P, Utens EM, Helbing WA *et al.* Unnatural history of tetralogy of Fallot: prospective follow-up of 40 years after surgical correction. *Circulation* 2014;**130**:1944–53.
5. Jang W, Kim YJ, Choi K, Lim HG, Kim WH, Lee JR. Mid-term results of bioprosthetic pulmonary valve replacement in pulmonary regurgitation after tetralogy of Fallot repair. *Eur J Cardiothorac Surg* 2012;**42**:e1–8.
6. Khairy P, Van Hare GF, Balaji S, Berul CI, Cecchin F, Cohen MI *et al.* PACES/HRS Expert Consensus Statement on the Recognition and Management of Arrhythmias in Adult Congenital Heart Disease: developed in partnership between the Pediatric and Congenital Electrophysiology Society (PACES) and the Heart Rhythm Society (HRS). Endorsed by the governing bodies of PACES, HRS, the American College of Cardiology (ACC), the American Heart Association (AHA), the European Heart Rhythm Association (EHRA), the Canadian Heart Rhythm Society (CHRS), and the International Society for Adult Congenital Heart Disease (ISACHD). *Heart Rhythm* 2014;**11**:e102–65.
7. Geva T. Repaired tetralogy of Fallot: the roles of cardiovascular magnetic resonance in evaluating pathophysiology and for pulmonary valve replacement decision support. *J Cardiovasc Magn Reson* 2011;**13**:9.
8. Broberg CS, Chugh SS, Conklin C, Sahn DJ, Jerosch-Herold M. Quantification of diffuse myocardial fibrosis and its association with myocardial dysfunction in congenital heart disease. *Circ Cardiovasc Imaging* 2010;**3**:727–34.
9. Kozak MF, Redington A, Yoo SJ, Seed M, Greiser A, Grosse-Wortmann L. Diffuse myocardial fibrosis following tetralogy of Fallot repair: a T1 mapping cardiac magnetic resonance study. *Pediatr Radiol* 2014;**44**:403–9.
10. Chen CA, Dusenbery SM, Valente AM, Powell AJ, Geva T. Myocardial ECV fraction assessed by CMR is associated with type of hemodynamic load and arrhythmia in repaired tetralogy of Fallot. *JACC Cardiovasc Imaging* 2016;**9**:1–10.
11. Riesenkampff E, Luining W, Seed M, Chungsomprasong P, Manlhiot C, Elders B *et al.* Increased left ventricular myocardial extracellular volume is associated with longer cardiopulmonary bypass times, biventricular enlargement and reduced

exercise tolerance in children after repair of Tetralogy of Fallot. *J Cardiovasc Magn Reson* 2016;**18**:75.
12. Yim D, Riesenkampff E, Caro-Dominguez P, Yoo SJ, Seed M, Grosse-Wortmann L. Assessment of diffuse ventricular myocardial fibrosis using native T1 in children with repaired tetralogy of Fallot. *Circ Cardiovasc Imaging* 2017;**10**.pii:e005695.
13. Oosterhof T, Mulder BJ, Vliegen HW, de Roos A. Corrected tetralogy of fallot: delayed enhancement in right ventricular outflow tract. *Radiology* 2005;**237**: 868–71.
14. Babu-Narayan SV, Kilner PJ, Li W, Moon JC, Goktekin O, Davlouros PA *et al*. Ventricular fibrosis suggested by cardiovascular magnetic resonance in adults with repaired tetralogy of fallot and its relationship to adverse markers of clinical outcome. *Circulation* 2006;**113**:405–13.
15. Oakes RS, Badger TJ, Kholmovski EG, Akoum N, Burgon NS, Fish EN *et al*. Detection and quantification of left atrial structural remodeling with delayed-enhancement magnetic resonance imaging in patients with atrial fibrillation. *Circulation* 2009;**119**:1758–67.
16. Stirrat J, Rajchl M, Bergin L, Patton DJ, Peters T, White JA. High-resolution 3-dimensional late gadolinium enhancement scar imaging in surgically corrected Tetralogy of Fallot: clinical feasibility of volumetric quantification and visualization. *J Cardiovasc Magn Reson* 2014;**16**:76.
17. Vittinghoff E, McCulloch CE. Relaxing the rule of ten events per variable in logistic and Cox regression. *Am J Epidemiol* 2007;**165**:710–8.
18. Broberg CS, Huang J, Hogberg I, McLarry J, Woods P, Burchill LJ *et al*. Diffuse LV myocardial fibrosis and its clinical associations in adults with repaired tetralogy of fallot. *JACC Cardiovasc Imaging* 2016;**9**:86–7.
19. Raman FS, Kawel-Boehm N, Gai N, Freed M, Han J, Liu CY *et al*. Modified look-locker inversion recovery T1 mapping indices: assessment of accuracy and reproducibility between magnetic resonance scanners. *J Cardiovasc Magn Reson* 2013; **15**:64.
20. Dobson RJ, Mordi I, Danton MH, Walker NL, Walker HA, Tzemos N. Late gadolinium enhancement and adverse outcomes in a contemporary cohort of adult survivors of tetralogy of Fallot. *Congenit Heart Dis* 2017;**12**:58–66.
21. Kapel GF, Sacher F, Dekkers OM, Watanabe M, Blom NA, Thambo JB *et al*. Arrhythmogenic anatomical isthmuses identified by electroanatomical mapping are the substrate for ventricular tachycardia in repaired Tetralogy of Fallot. *Eur Heart J* 2017;**38**:268–76.
22. Geva T, Sandweiss BM, Gauvreau K, Lock JE, Powell AJ. Factors associated with impaired clinical status in long-term survivors of tetralogy of Fallot repair evaluated by magnetic resonance imaging. *J Am Coll Cardiol* 2004;**43**:1068–74.
23. Friedberg MK, Redington AN. Right versus left ventricular failure: differences, similarities, and interactions. *Circulation* 2014;**129**:1033–44.
24. Bokma JP, Winter MM, Kornaat EM, Vliegen HW, van Dijk AP, van Melle JP *et al*. Right vEntricular Dysfunction in tEtralogy of Fallot: iNhibition of the rEnin-angiotensin-aldosterone system (REDEFINE) trial: rationale and design of a randomized, double-blind, placebo-controlled clinical trial. *Am Heart J* 2017;**186**: 83–90.
25. Oosterhof T, van Straten A, Vliegen HW, Meijboom FJ, van Dijk AP, Spijkerboer AM *et al*. Preoperative thresholds for pulmonary valve replacement in patients with corrected tetralogy of Fallot using cardiovascular magnetic resonance. *Circulation* 2007;**116**:545–51.
26. Bricker JT. Sudden death and tetralogy of Fallot. Risks, markers, and causes. *Circulation* 1995;**92**:158–9.
27. Garson A Jr, Randall DC, Gillette PC, Smith RT, Moak JP, McVey P *et al*. Prevention of sudden death after repair of tetralogy of Fallot: treatment of ventricular arrhythmias. *J Am Coll Cardiol* 1985;**6**:221–7.
28. Meierhofer C, Tavakkoli T, Kühn A, Ulm K, Hager A, Müller J *et al*. Importance of non-invasive right and left ventricular variables on exercise capacity in patients with tetralogy of fallot hemodynamics. *Pediatr Cardiol* 2017;**38**:1569–74.
29. Woudstra OI, Bokma JP, Winter MM, Kiès P, Jongbloed MRM, Vliegen HW *et al*. Clinical course of tricuspid regurgitation in repaired tetralogy of Fallot. *Int J Cardiol* 2017;**243**:191–3.
30. Chang MC, Wu MT, Weng KP, Su MY, Menza M, Huang HC *et al*. Left ventricular regional myocardial motion and twist function in repaired tetralogy of Fallot evaluated by magnetic resonance tissue phase mapping. *Eur Radiol* 2017;**28**: 104–14.
31. Orwat S, Diller GP, Kempny A, Radke R, Peters B, Kühne T *et al*. Myocardial deformation parameters predict outcome in patients with repaired tetralogy of Fallot. *Heart* 2016;**102**:209–15.